CZECH TECHNICAL UNIVERSITY IN PRAGUE

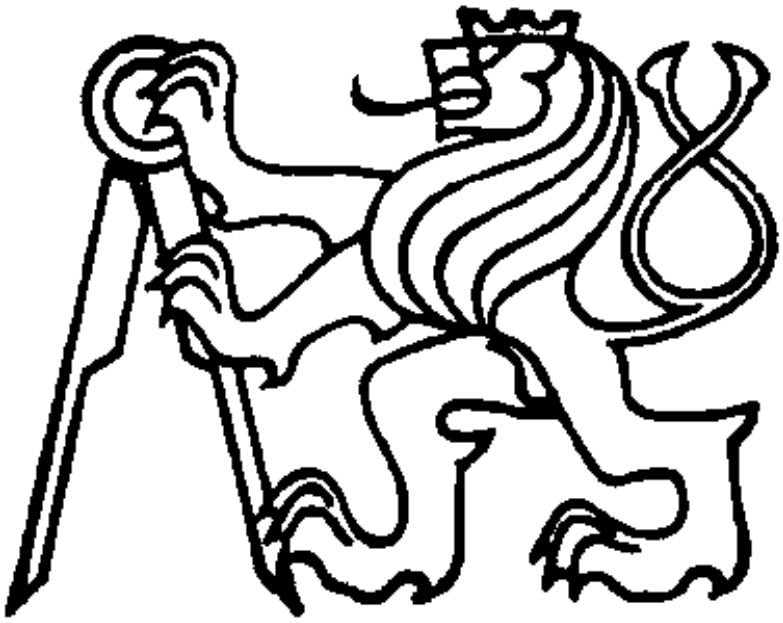

DOCTORAL THESIS STATEMENT

Czech Technical University in Prague

Faculty of Electrical Engineering

Department of Physics

Ing. Petr Hoffer

SHOCK WAVES GENERATED BY CORONA-LIKE DISCHARGES IN WATER

Ph.D. Programme: Electrical Engineering and Information Technology

Branch of study: Plasma Physics

Doctoral thesis statement for obtaining the academic title of "Doctor", abbreviated to "Ph.D."

Prague, June 2014

The doctoral thesis was produced in part-time manner

Ph.D. study at the department of Physics of the Faculty of Electrical Engineering of the CTU in Prague

Candidate: **Ing. Petr Hoffer**
Pulse Plasma Systems
Institute of Plasma Physics AS CR, v.v.i.
Za Slovankou 1782/3, 182 00 Prague 8

Supervisor: **Doc. Ing. Pavel Šunka, CSc.**
Pulse Plasma Systems
Institute of Plasma Physics AS CR, v.v.i.
Za Slovankou 1782/3, 182 00 Prague 8

Supervisor-Specialist: **Prof. RNDr. Pavel Kubeš, CSc.**
Faculty of Electrical Engineering of the CTU in Prague
Technická 2, 166 27 Prague 6

Opponents: **……**

……

……

…….

……

The doctoral thesis statement was distributed on: ……

The defence of the doctoral thesis will be held on …….. at ……. a.m./p.m. before the Board for the Defence of the Doctoral Thesis in the branch of study Plasma Physics in the meeting room No. …..... of the Faculty of Electrical Engineering of the CTU in Prague.

Those interested may get acquainted with the doctoral thesis concerned at the Dean Office of the Faculty of Electrical Engineering of the CTU in Prague, at the Department for Science and Research, Technická 2, Praha 6.

Chairman of the Board for the Defence of the Doctoral Thesis
in the branch of study Plasma Physics
Faculty of Electrical Engineering of the CTU in Prague
Technická 2, 166 27 Prague 6.

Contents

1. Introduction, review

Although electric discharges in water have been studied for many years, processes of formation and propagation of the discharges in water volume has not been fully understood yet. The propagation of the discharges in water is often accompanied by generation of shock or pressure waves. ***The breakdown mechanism in liquids*** is more complicated than that in gases, because liquids are much denser. There are several different breakdown mechanisms that cannot be described in the context of a unified theory. At least five different mechanisms of the discharge initiation can be identified. (1) The *microexplosive* liquid discharge initiation mechanism is based on the electron emission into liquid [1] (in the case of discharge from the cathode) or on the ionization of liquid molecules (in the case of discharge from the anode) [2, 3, 4]. Current of induced charge carriers quickly heats up the liquid, that starts to expand and a shock wave is formed. Explosive vaporization of the liquid is accompanied by breakdown of vapor bubbles. (2) The *ionization* liquid discharge initiation mechanism, similarly as microexplosive mechanism, is based on autoionization of liquid molecules (anode initiation) or collision ionization (cathode initiation) [2, 3]. The difference is that the liquid-vapor phase transition is not necessary for the discharge initiation. The ionization processes occur at the density of liquid phase. (3) The *electrostrictive* liquid discharge initiation is based on violation of liquid continuity in the vicinity of a sharp electrode (or bulge) due to the effective negative pressure caused by electrostrictive ponderomotive force pushing dielectric fluid to the regions with higher electric field [5, 6, 7]. When stretching electrostrictive pressure ruptures a liquid, expanding bubbles naturally appear in region with strong electric field. These low-density cavities effectively facilitate electron avalanche sufficient to initiate breakdown [8]. (4) The *electrothermal* and (5) *bubble* mechanism of liquid discharge initiation is based on breakdown of bubbles created by boiling of a conductive liquid, or on breakdown of bubbles that already existed on the electrodes and in a non-degassed liquid before field application [3].

Propagation of plasma ignited on the surface of initiating electrode toward the opposite electrode may be realized in several different forms, most often as plasma streamers. Low current stagnating or propagating electric discharges in liquids (not sparks between electrodes) are generally called *corona-like discharges*.

When gas discharge in a bubble on electrode surface is ignited, it elongates toward the opposite electrode. This type of discharge propagation is the slowest one. After breakdown a constricted glow-like discharge in a bubble is observed. Such bubbles elongate from the spot, where the gas plasma attaches to the bubble wall. More information about discharges in bubbles can be found in [9, 10, 11].

Non-luminous *primary streamers* are often the early stadium of ***positive streamers*** propagating in water, which can, but need not start to propagate from an initial gas bubble with plasma streamers inside. The launch of primary streamers is triggered, when local electric field is of the order of 10^8 MV·m^{-1} [12]. Primary discharges have hemispherical bush-like appearance, where the edges of the individual streamers can be clearly resolved (their channel diameters were measured to be 3-10 μm [13]), and propagate along radial directions at relatively low velocities (often subsonic, but some may reach even several kilometers per second) producing spherical shockwaves. When the electric field at the tip of one of the primary streamer becomes high enough, *secondary streamers* can be formed [14, 12, 3]. While propagation of primary streamers is often subsonic (in water it means speed smaller than ~1.5 km·s^{-1}), propagation speed of secondary streamers can be of the order of 100 km·s^{-1} [13]. Field induced dissociation and ionization of molecules in the bulk liquid are considered as basic mechanisms for secondary streamer propagation, because electric field around the secondary streamer heads reaches 2 GV·m^{-1} [12].

Negative streamers readily emerge from the discharges in bubbles. They do not exhibit the hemispherical shape as the positive primary streamers do, but they are more bush-like. They have a smaller propagation velocity at moderate voltages (< 400 $m \cdot s^{-1}$) [14], but their propagation may be even supersonic. Propagation velocity of negative streamers is independent on the water solution conductivity [15]. Negative streamers in water with higher conductivities are much thicker (the characteristic diameter of negative streamers in distilled water is as large as 50 μm) and decrease in their length [14].

The existence of ***shockwaves*** around discharges in water is very well known (e.g. in [13, 14, 16, 17, 3]), but there is just the only one article [12] containing analysis of pressure field around *positive corona-like discharges*, specifically, pressure field around positive secondary streamers in distilled water or in low conductive aqueous solution. The authors distinguished two kinds of streamers: active and inactive. Active streamers are propagating, when the diagnostic laser is triggered. Active streamers could be recognized by a conical shape (Mach cone) of the shock front evolving from them. Inactive streamers have (nearly) stopped propagating, therefore, a spherical shape of the pressure wave at the streamer head is observed. The peak pressure of the shock front of an inactive streamer, when it has reached radius of 35 μm, is 46 MPa. The streamer propagation speed has been found to be 25 $km \cdot s^{-1}$.

Shockwaves generated by *negative coronas* are generally weaker, because the negative streamers are often subsonic. Thus, spherical shockwaves or weak pressure waves instead of Mach cones are emitted from the tip of each propagating streamer. The waves are not emitted from sides of negative streamers [16], as it is in the case of positive streamers.

High number of corona-like discharges can be produced by using of so called *composite electrodes*. The composite electrodes have been developed and used in the Institute of Plasma Physics AS CR in generators of focused shockwaves, which are described in more detail in [18, 19, 20, 21]. In this device, a primary cylindrical diverging pressure wave, generated by the underwater multichannel pulsed corona-like discharge, is after reflection on parabolic reflector theoretically transformed to semi-spherical converging pressure wave that near the reflector focus subsequently changes by natural distortion into a shock wave. Analyses of focused shockwaves produced by this generator and diagnosed by obsolete methods can also be found in the above mentioned articles.

2. Aims of the thesis

Propagation of plasma channels in water has not been fully explained yet. It has been said that ionization of molecules in bulk liquid by electric field of the order of $GV \cdot m^{-1}$ is responsible for high propagation speed of secondary streamers. Question is what process on a plasma-liquid boundary causes development of so tiny structures producing so strong electric field. Although all the mentioned mechanisms of discharge initiation in water require presence of strong electric field in liquid (10^8 $V \cdot m^{-1}$; in the case of ionization mechanism it is even 10^9 $V \cdot m^{-1}$), it does not mean that the secondary streamers utilizing ionization of liquid water for their propagation must be initiated by a needle electrode producing comparable electric field around its tip. Even discharges initiated on electrodes in relatively large bubbles can transform to secondary streamers with time.
The first aim of the thesis is studying of transitions of gas discharge in contact with surface of liquid electrode (distilled water, or a conductive water solution) to a streamer discharge in the liquid volume.

As it has been said in the previous review, an analysis of shockwaves around positive secondary streamers has been only done.
The second aim is analysis of pressure field produced by corona-like discharges burning in distilled water (especially primary streamers and negative streamers) and in conductive salt aqueous solutions at both polarities. It includes discharges on needle electrodes as well as discharges on composite electrodes.

The third aim is analysis of pressure field at focal area of the generator of focused shockwave utilizing cylindrical composite anode as a source of multichannel corona-like discharge.

3. Working methods

Experimental setup 1

Transition of gas discharge in contact with surface of liquid electrode was not studied in gas phase within a bubble (where initial discharge often occurs), but the bubble inner surface was imitated by a meniscus of liquid water inside a glass capillary instead. High-speed shadowgraphy was used for the study.

The experimental setup is schematically depicted in the Figure 1. The power supply consisted of a high voltage capacitor *C* (10 - 400 nF), which was charged up to 50 kV by a high voltage DC power supply (not shown in the Fig. 1). The discharge current was limited by a high voltage resistor 10 kΩ protecting the used glass capillary from damage just in the case of liquid breakdown. Next, a pressurized spark gap was used as the high voltage switch. The investigated object (simulating bubble-water interface) consisted of the glass capillary, which was from the bottom side filled with the conductive water solution, while its upper end remained opened. The opened end was connected by a pipe to a vacuum pump or to a nitrogen/argon cylinder. The upper high voltage electrode was placed closely above the liquid surface, the lower, grounded one was immersed in the liquid solution at the sealed end of the capillary. The voltage across the electrode gap was measured by a high voltage probe, and the discharge current was calculated from the voltage on 1 Ω resistor. Both voltage signals were measured by an oscilloscope, which was triggered by the rising/falling edge of the signal from the high voltage probe. The oscilloscope then directly triggered the fast camera (max. 10^5 frames per second). The fast camera enables recording in the infinite loop regime, which means, that the output recording contains frames captured before the camera trigger as well as frames after that. The illumination of the capillary was provided either by a white light bulb (15 W), which allowed distinguishing of the discharge colors, or by a green power LED (12 W), the higher light-power output of which allowed using of higher camera frame-rate (requiring shorter exposure time).

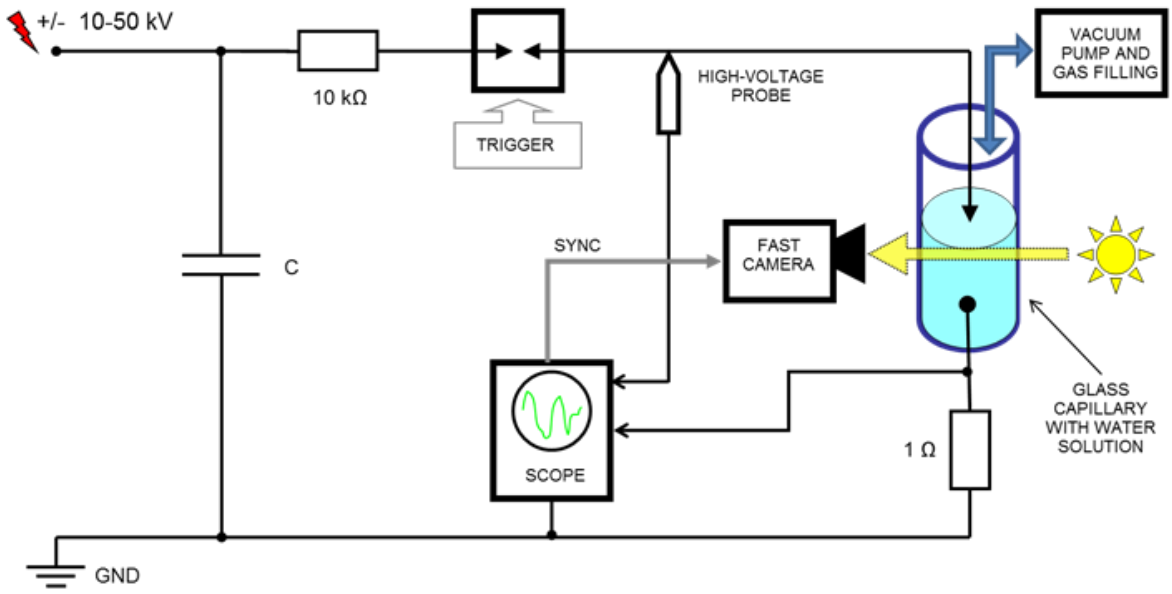

Figure 1 The experimental setup of the apparatus used for studying discharge passing through the surface of liquid water solution in a glass capillary.

Experimental setup 2

Studies of the pressure field in vicinity of corona-like discharges in distilled water and in highly conductive NaCl water solutions with conductivities up to 4 $S \cdot m^{-1}$ were performed in a different arrangement with a Mach-Zehnder interferometer as a main diagnostic tool. Namely the glass capillary was changed for a glass cuvette with plan-parallel windows. The experimental setup of the second experiment is depicted in the Figure 2. The pulse power supply was based on the same principle as in the first experiment; it consisted of a high voltage capacitor *C*, which was charged up to 50 kV by a high voltage DC power supply. The discharge current had to be limited by a resistor *R* protecting the used cuvette from damage just in the case of liquid breakdown. The pressurized spark gap was used as a high voltage switch again. The investigated volume consisted of the uncovered glass cuvette, which was filled with the liquid. The high voltage electrode was immersed in the liquid; it was stainless-steel wire insulated with exception of the sharpened tip. The lower, grounded electrode was formed by a stainless-steel slab, which also formed the base of the cuvette. The voltage across the electrode gap was measured by the high voltage probe, and the discharge current was measured by the current monitor (Pearson probe). Both voltage and current signals were registered by the oscilloscope, which was triggered by the rising/falling edge of the signal from the high voltage probe. Voltage on the 10 Ω resistor was used for indirect triggering of the high-speed camera. The Mach-Zehnder interferometer used the 532 nm pulsed laser (6.2 µJ/1.76 ns, maximum repetition rate $5 \cdot 10^4$ s^{-1}) as a source of coherent radiation. Diameter of the beam splitters was of ∅65 mm. Image on the camera CMOS chip was created by a set of lenses with diameter of ∅80 mm, and with the total focal length of 107 mm. The distance between the cuvette and the set of lenses was set to the smallest achievable distance of 149 mm; this enabled the lenses to collect the maximum of light bended on strong inhomogeneities in the liquid filling of the cuvette. The high-speed camera was equipped with the interference filter tuned on the laser wavelength 532 nm, which suppressed most of the light emitted by the discharge.

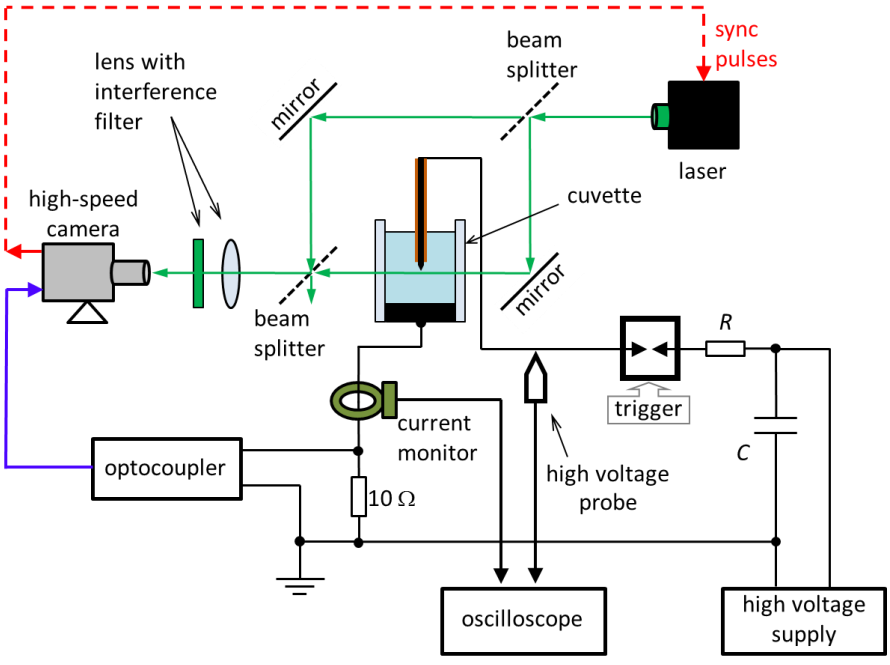

Figure 2 Experimental setup of the apparatus used for detection of pressure field around corona-like discharges in liquid water solution in a glass cuvette.

Experimental setup 3

The pressure field in the focal area of the generator of focused waves was investigated in a totally different apparatus shown schematically in the Figure 3. The shock wave generator consists of a cylindrical high-voltage composite anode placed along the axis of the outer metallic parabolic reflector (cathode) [19]. The cylindrical composite electrode has ∅60 mm diameter and 100 mm length. The focal point of the parabolic reflector is 70 mm above the reflector's aperture. The pulse power supply consists of a high voltage DC source, a low inductance high voltage pulse capacitor of 0.8 μF, and a spark gap switch. The electrode system is immersed in a conductive aqueous salt solution (1.8 $S \cdot m^{-1}$). A high voltage pulse of positive polarity with amplitude of 21 kV was applied to the composite electrode. Pressure measurements were performed using a fiber optic probe hydrophone (FOPH). Tip of the FOPH was placed in the generator's focal area, and signals from the FOPH's photo-detector were captured by a digital oscilloscope. An ultra-high-speed camera (10^6 frames per second) and a flash lamp were used for high speed real-time shadowgraph visualization of shock wave propagation and focusing in the focal area. A Pearson probe current monitor was used as a source of trigger signal. This signal directly triggered the oscilloscope and a delay unit, which was used to synchronize the timing of the flash lamp and the camera.

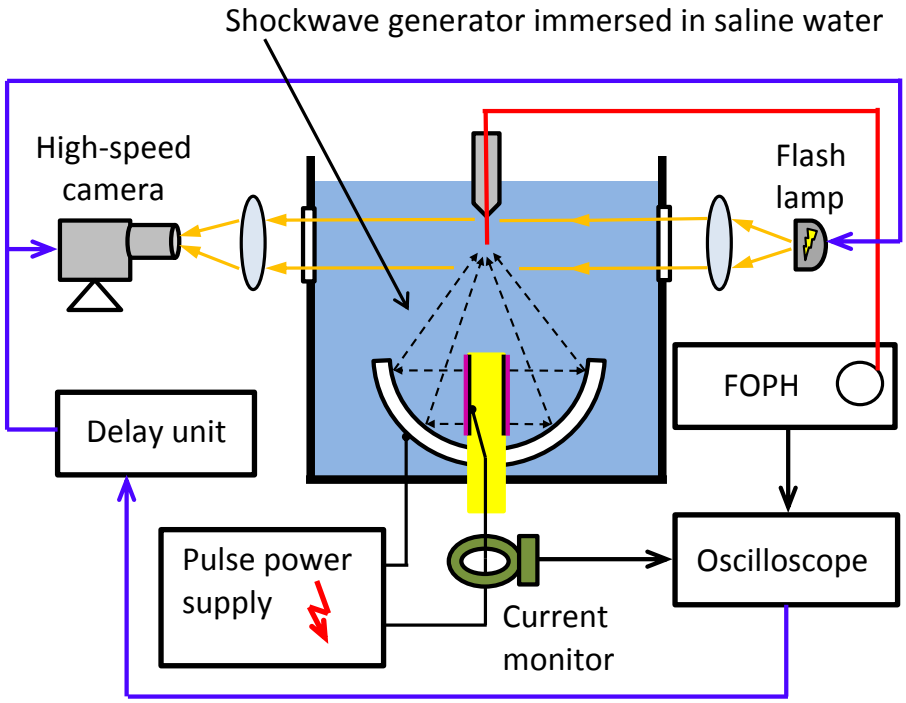

Figure 3 The experimental setup of the apparatus used for analysis of pressure field in the focal area of the shockwave generator.

4. Results

1. Streamer development

Figure 4 demonstrates evolution of the negative streamer in a short (10 mm) liquid column at current 100 mA. Tiny dips with diameter of about 50 μm early appear at the liquid surface. These dips are pointed by black arrows in the second frame (in 94 μs). Very fine negative streamer then grows from one of the dips at the initial speed of 93 $m \cdot s^{-1}$. It reaches anode in 157 μs and causes capillary breakdown accompanied by a significant increase of the current.
It seems that plasma conductivity (above water surface) to water conductivity ratio may be the

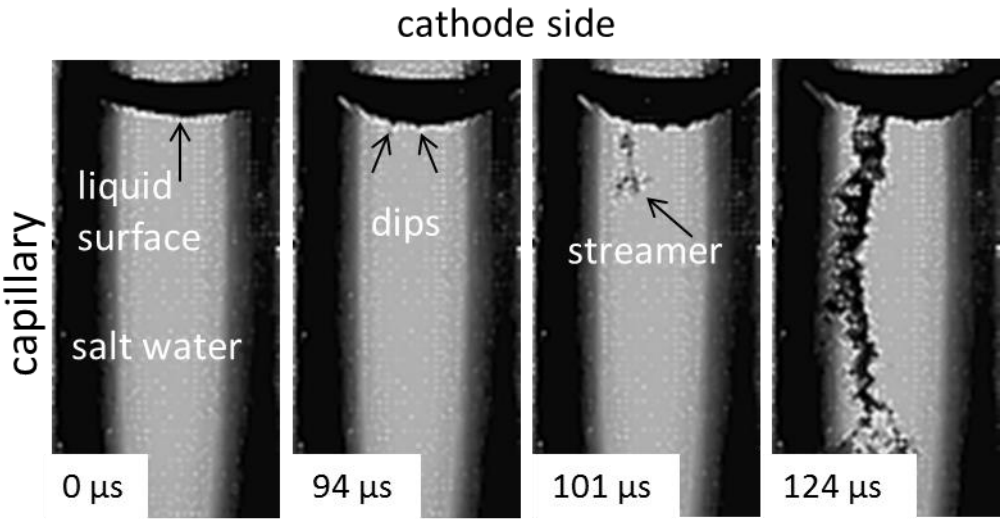

Figure 4 The negative streamer in salt water anode in glass capillary; parameters are: liquid column height 10 mm, capillary diameter 2 mm, voltage 20 kV, water solution conductivity 18 $mS \cdot m^{-1}$.The metal (copper) electrodes are not visible; the cathode was placed just above the meniscus surface (gas discharge connected the electrode with the liquid surface).

key factor, which decides, if water-surface is smoothened and dug in large area, or if water surface is dug locally in places of inception dips – that results in formation of narrow tunnels of negative streamers. If plasma conductivity is higher than liquid conductivity, the distribution of the current density on the plasma-liquid boundary will be unstable due to liquid evaporation. Any initial surface disturbances boost the current density in surface valleys causing simultaneously a detriment of the surrounding current density (see the Figure 6a). Consequent stronger liquid evaporation from the valleys causes their deepening, and hence, next enhancement of the current density distribution inhomogeneity. In the opposite situation (see the Figure 6b), the liquid conductivity is higher than the plasma conductivity. Although the current density on the cone vertex is higher than that in the previous case, the current density on the edge of the cone basement (edge of the dip) is four times higher than the current density on the vertex. This results in more intense evaporation of liquid from the surrounding of the inception dip than from its vertex, and hence, in smoothing of the liquid surface instead of the dip deepening. The overall intensity of evaporation from the liquid surface have no influence on the surface-streamer transition.
Experiments with liquid cathode showed also creation of spikes similar to the dips on the liquid surface, which worked often as streamer predecessors in the case of the liquid anode. These spikes do not emerge from calm liquid surface as the dips do; they develop from more extensive surface deformations only. In the case of liquid cathode no spike-streamer transition occurs, unless the initial electric field on the liquid surface is high enough. The spikes appear in places of the next cavity elongation. Similarly to dips in the case of the liquid anode, the

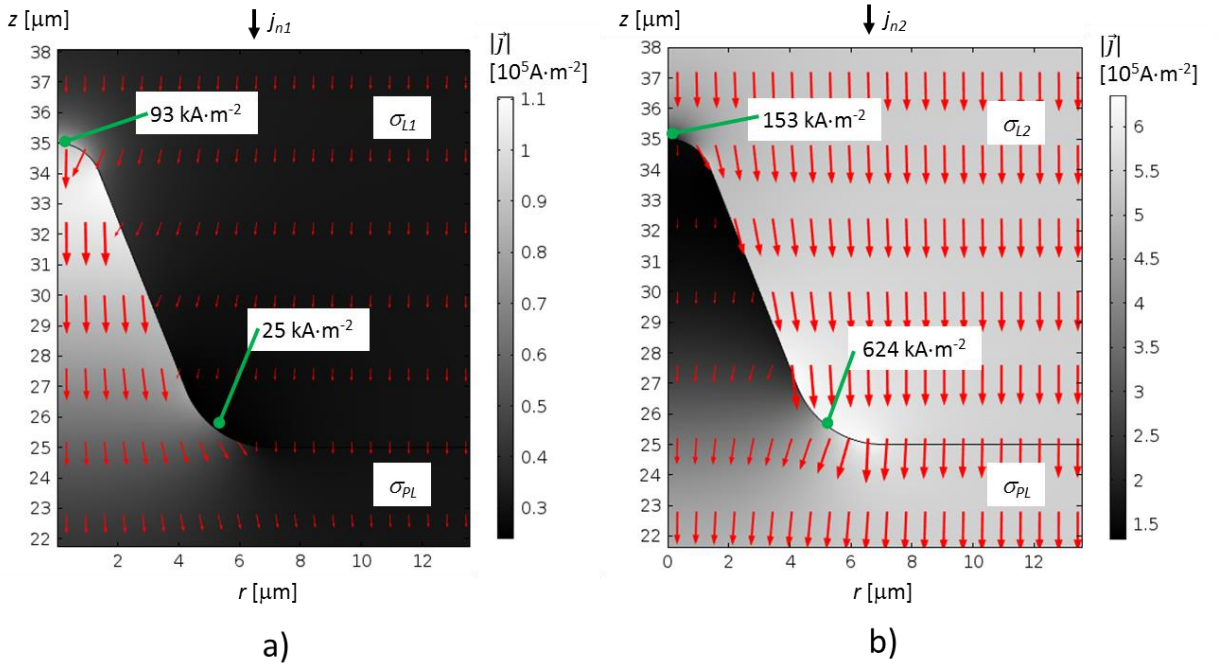

Figure 6 Stationary simulation of current density distribution in the place of a small perturbation of plasma-liquid boundary. Liquid conductivities were **a)** σ_{L1} = 18 mS·m^{-1}, **b)** σ_{L2} = 300 mS·m^{-1} and the plasma conductivity was in both cases σ_{PL} = 74.5 mS·m^{-1}; initial boundary normal current densities were **a)** j_{n1} = 31.8 kA·m^{-2} and **b)** j_{n2} = 541 kA·m^{-2}. The simulation was performed using Comsol Multiphysics software with liquid at the top and plasma at the bottom.

spikes develop only in the liquid cathode with relatively low conductivity. Surface-secondary streamer transition happens only if initial high electric field of the order of 10 MV·m^{-1} is present on the liquid surface.

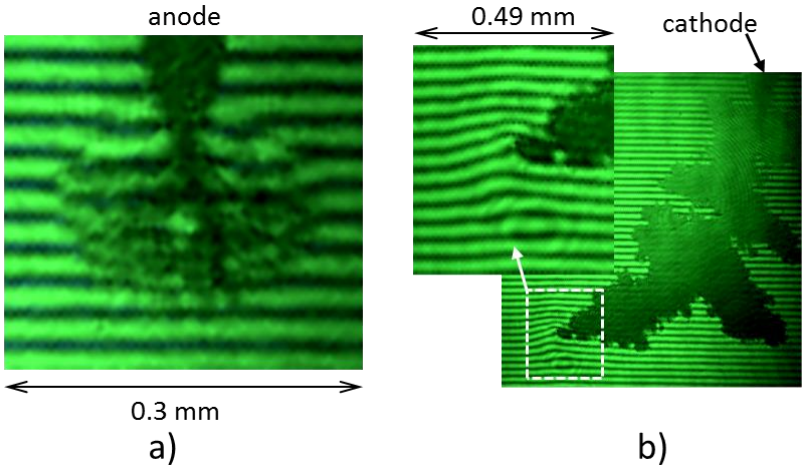

Figure 5 Interferograms of **a)** surroundings of a primary positive discharge, **b)** surroundings of a negative discharge with the detail of the streamers tip.

2. Analysis of pressure field around corona-like discharges

Pressure field around corona-like discharges in *distilled water* and in salt water solutions with different conductivities have been analysed. Shockwave with peak pressure of 33 MPa were detected around primary positive streamers in distilled water (Figure 5a) and some of them

were obviously supersonic. Contrary, streamers of negative corona-like discharge in distilled water do not produce shockwaves at all, only slightly elevated (10–20 MPa) pressure area was found around streamer tip, which points to subsonic propagation velocity of these streamers (Figure 5b).

In the case of positive discharges in *conductive salt solution*, fringes at lower conductivities could not be recognized due to high complexity of pressure field. Simpler pressure fields appears at the highest used conductivities (1.8, and 3.8 $S \cdot m^{-1}$) only: it has form of spherical pressure wave with radius ~1 mm, thickness of transition region ~200 μm, and peak pressure 18-20 MPa (Figure 7a). Since the discharge currents at these conductivities are comparable, similarly as the generated pressure levels are, it was deduced that the plasma conductivities of these discharges have to be also similar, and independent on conductivity of the salt solutions. At the highest conductivity the streamers recede (remaining only as signs of streamers), and the pressure waves are generated rather by expanding bumpy cavity.

No streamers appear in the case of negative discharges in salt solutions with conductivity $\geq 0.4\ S \cdot m^{-1}$. An expanding spherical cavity occurrs instead; and this cavity produces a spherical pressure wave. It was found that at solution conductivities of 0.4 and 0.8 $S \cdot m^{-1}$ the dependence of wave peak pressure (~4 MPa) on current is insignificant. However, at conductivity of 1.8 $S \cdot m^{-1}$ (Figure 7b) the peak pressure increases nearly twice (when converted to the same radius) and reaches 9 MPa at the wave radius of 0.5 mm. At conductivity of 3.8 $S \cdot m^{-1}$ the peak pressure falls down to only 3 MPa at the wave radius of 0.5 mm.

Numerical simulations were performed to find such temporal development of the radial velocity of the expanding discharge cavity, which produced a similar pressure profile as that detected by interferogram taken in one not exactly specified moment around discharges in the solution with conductivity of 1.8 $S \cdot m^{-1}$. A qualified estimate based on this simulation gives plasma conductivity of the order of ~1 $S \cdot m^{-1}$ – i.e. value comparable with surrounding solution conductivity. The simulation has also shown that in the beginning the cavity expands very slowly and does not generate any pressure wave, however, as soon as the cavity reaches radius ~100 μm, it starts rapidly to expand and generate the pressure wave.

Results of experiments focused on analyses of pressure waves produced by corona-like discharges on composite anode (Figure 8) show that radial pressure profile of a typical semi-spherical wave with radius of 440 μm has a front jump up to ~8 MPa with thickness of the transition region of 12 μm. Behind this jump the pressure monotonically increases up to 21 MPa. Since about 100 discharges burning on 100 mm^2 of composite anode have together

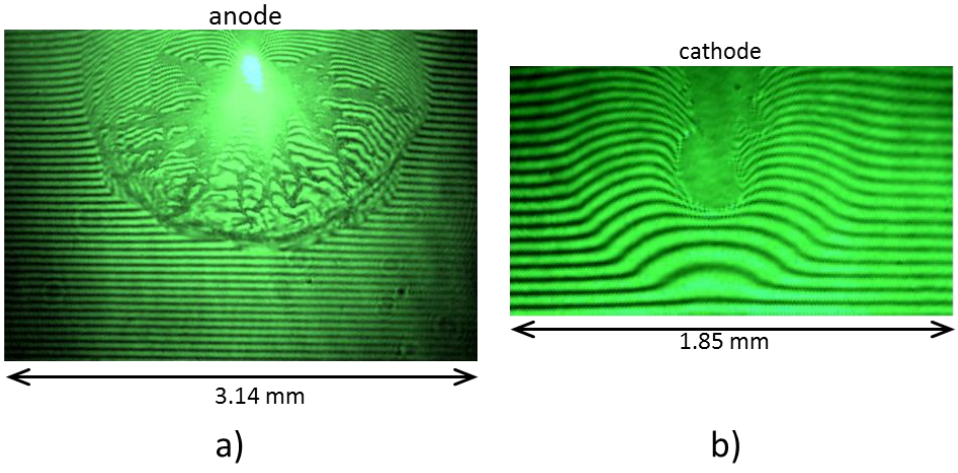

Figure 7 Interferograms of **a)** surroundings of a positive discharge, **b)** surroundings of a negative discharge. Liquid conductivity was 1.8 $S \cdot m^{-1}$.

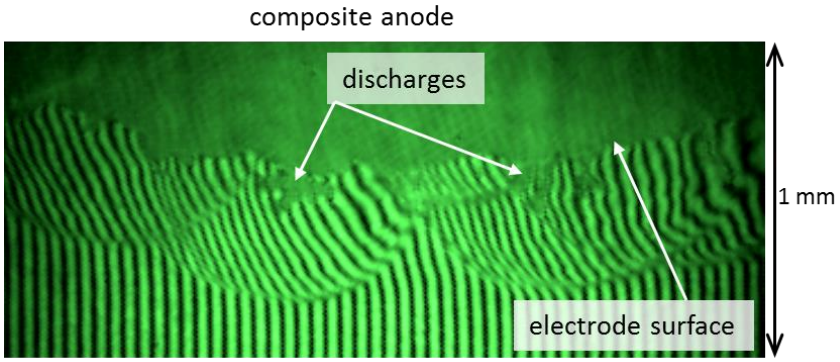

Figure 8 Interferogram of the surroundings of positive corona-like discharges produced on composite anode in salt water solution with conductivity 1.8 $S \cdot m^{-1}$.

the same current as the discharge on one needle electrode (at the same liquid conductivity) and since one individual discharge on a composite anode generates practically the same pressure as the discharge on the needle electrode, it is possible to conclude that the production of pressure waves by composite electrode is much more efficient than production by needle electrode.

Pressure profile of spherical pressure waves generated by discharges on composite cathode monotonically increases from its outer radius to the inner one without any jump reaching the pressure of 20 MPa near the composite cathode surface.

The individual semi-spherical pressure waves generated by discharges on both composite anode and cathode are often not produced simultaneously, probably because of different filling of individual pores (Figure 9).

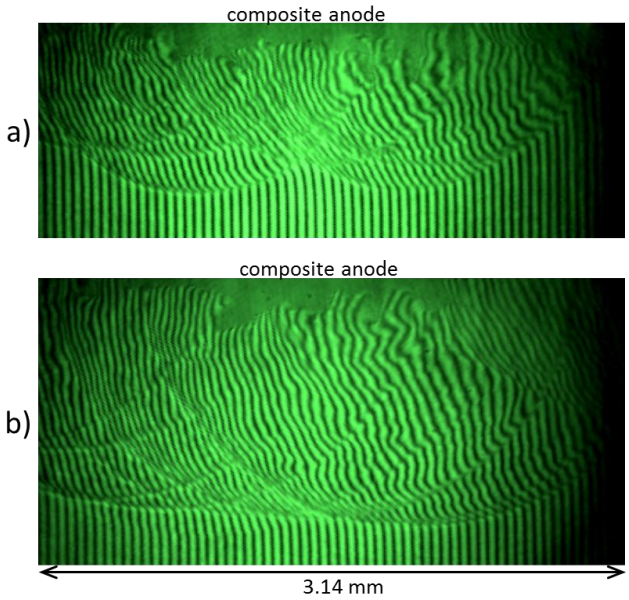

Figure 9 Interferograms of the surroundings of positive corona-like discharges produced on composite anode in salt water solution with conductivity 1.8 $S \cdot m^{-1}$; **a)** discharges were initiated in different times, emitted pressure waves have different radii; **b)** discharges were initiated simultaneously, emitted pressure waves have nearly the same radii, and their outer boundaries form a uniform envelope.

3. Analysis of focused shockwaves generated by multichannel corona-like discharge

The generation and focusing of shock waves excited by the multichannel corona-like discharge system with the composite cylindrical anode has been investigated. Experiments showed that expanding cylindrical pressure wave produces after reflection from the generator reflector an intersecting conical shock wave travelling along the axis of symmetry of the reflector (Figure 10). In the focal plane (7.5 mm further than the geometric focus of the

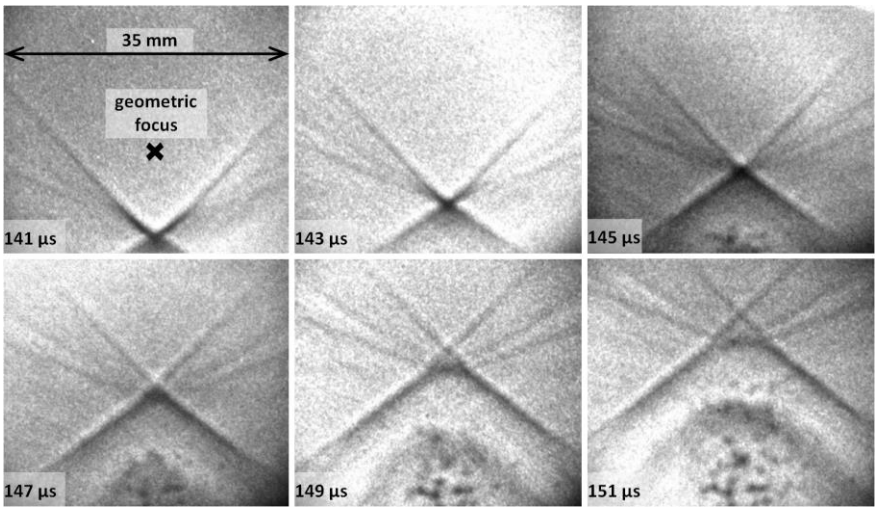

Figure 10 Selected real-time shadowgraph images of shock wave propagation through the focal area. The shock wave propagated from the bottom to the top of the frame.

reflector) the pressure amplitudes of the shock wave rapidly decrease with radial distance *R* from the focus (~0.25 mm), and the pressure waveforms significantly change with *R* (Figure 11). The maximum measured peak pressure of the focused shock wave was 372 MPa, averaged over the area of the FOPH (100 µm in diameter). The propagation velocity of the conical shock front in its normal direction was 1.51 ± 0.1 km·s^{-1}. The propagation velocity of the intersection point of the conical shockwave on the axis of symmetry was 2.17 ± 0.1 km·s^{-1}.

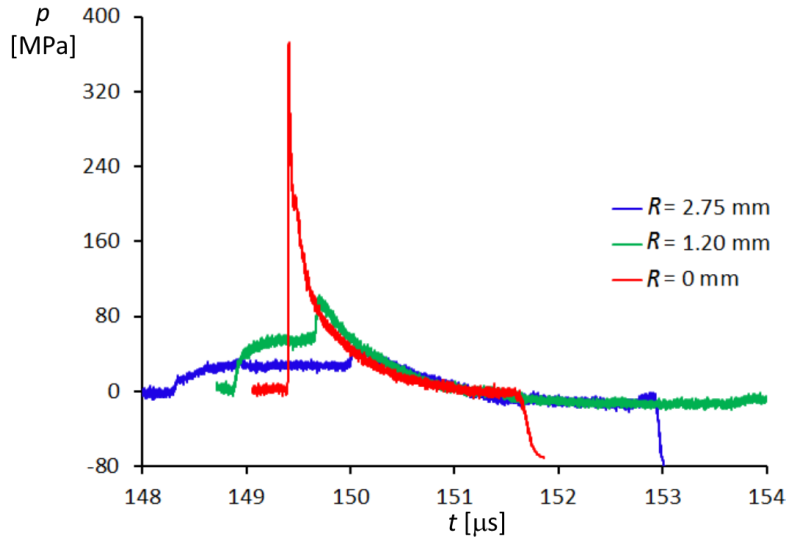

Figure 11 Shock wave pressure waveforms measured by the FOPH at three different radial distances (*R*) from the focus.

Conclusion

One of the most frequent initiation mechanisms of underwater discharges is an electrical breakdown of bubbles on a metallic electrode, from which the discharge penetrates (through limited area of bubble-water interface) into liquid volume. This situation was simulated by experiments with so called *liquid anode* and *cathode* in glass capillaries. The experiments were aimed at studies of above mentioned ***penetration of plasma*** from the limited liquid surface (meniscus in the capillary) ***into the liquid volume***. High speed shadowgraphy was used as the main diagnostic tool.

Experiments with *liquid anodes* showed, that liquid surface in the place of the largest current density (at the plasma-liquid interface) recedes. This receding is caused by reaction pressure resulting from liquid evaporation. Thus, long cavities with plasma inside can be formed or even can cause the total electrical breakdown. Propagation speed of the elongating cavity-wall is of the order of 1 $m \cdot s^{-1}$, and it depends on current density. The liquid surface of the meniscus or cavity remains smooth when the liquid conductivity is larger than the conductivity of adjacent plasma. In the opposite case, the distribution of the current density on the plasma-liquid boundary is unstable due to liquid evaporation. Any initial surface disturbances boost the current density in surface dents causing simultaneously a detriment of the surrounding current density. Consequent stronger liquid evaporation from the dents causes their deepening, and hence, next enhancement of the current density distribution inhomogeneity. The dips created by this way subsequently elongate, and often fluently transform into negative streamers, when electric field larger than 1 $MV \cdot m^{-1}$ appears near the liquid surface. Negative streamers propagate toward the immersed metal anode at subsonic speed of the order of 100 $m \cdot s^{-1}$.

Experiments with *liquid cathodes* showed significantly more intense liquid evaporation than the experiments with liquid anodes – under otherwise the same conditions. Therefore, elongation speed of gas cavities is also significantly higher. Although the development of spikes on the liquid surface is also determined by the ratio of plasma-liquid conductivities, it is followed by transition to secondary positive streamers only when larger electric field than 10 $MV \cdot m^{-1}$ appears near the liquid surface.

Experiments with corona-like discharges on needle and composite electrodes in aqueous salt solutions with different conductivities were aimed at interferometry ***analysis of pressure field*** around these discharges. It has been found that pressure waves generated by positive coronas reach generally higher pressure levels.

Profile of spherical shockwave generated by primary discharge on *positive needle electrode* in distilled water was successfully analyzed. The shock front represents boundary of the driving fan-shaped primary streamer discharges; its pressure amplitude reaches 30 MPa at the wave radius 100 μm. Experiments with positive discharges in salt aqueous solutions showed high volume number density of positive streamers at conductivities 0.4 and 0.8 $S \cdot m^{-1}$, which did not allow to recognize fringes in the captured interferograms. Spherical pressure waves around positive discharges in solutions with higher conductivities - 1.8 and 3.8 $S \cdot m^{-1}$ enabled pressure analysis yielding pressure amplitude in both cases 20 MPa at the wave radius 1 mm. Since the discharge currents at these conductivities (1.8 and 3.8 $S \cdot m^{-1}$) were comparable, similarly as the generated pressure levels, it has been concluded that the plasma conductivity of the discharges had to be similar, and independent on conductivity of the salt solutions. At the highest conductivity (3.8 $S \cdot m^{-1}$) streamers receded, and the pressure waves were generated rather by expanding bumpy cavity with only signs of streamers.

Profile of spherical pressure wave generated by discharge on *negative needle electrode* in distilled water was also successfully analyzed. Maximum amplitude of pressure waves formed on tip of negative streamers in distilled water reaches 20 MPa. However, the pressure profile contains no sharp discontinuity, which bears witness to subsonic propagation speed.

No streamers appear in the case of negative discharges in salt solutions with conductivity $\geq 0.4\ S \cdot m^{-1}$. Instead, an expanding nearly spherical cavity occurs and produces spherical pressure wave. Dependence of the wave peak pressure on current has been found to be insignificant at lower solution conductivities (0.4 and $0.8\ S \cdot m^{-1}$). The peak pressure reaches 4 MPa (wave radius ~0.5 mm) at these conductivities. However, at conductivity of $1.8\ S \cdot m^{-1}$ the peak pressure reaches ~9 MPa (wave radius ~0.5 mm). At conductivity of $3.8\ S \cdot m^{-1}$ the peak pressure falls back to only ~3 MPa (wave radius ~0.5 mm).

Numerical simulations were performed to find such temporal development of the radial velocity of the expanding discharge cavity, which produces a similar pressure profile as that detected around discharges on negative needle electrode in the salt solution with conductivity of $1.8\ S \cdot m^{-1}$. The simulations and experiments also showed that in the beginning the cavity expands so slowly that this expansion does not generate any pressure wave; however, as soon as the cavity radius reaches ~100 μm the situation is just opposite: a rapid cavity expansion occurs and is accompanied by generation of strong pressure wave.

Analysis of interferogram of corona-like discharges burning on *composite anode* in aqueous salt solution with conductivity of $1.8\ S \cdot m^{-1}$ showed that radial pressure profile of a typical semi-spherical pressure wave (due to the discharge from a single pore) with radius of 440 μm has on its front a pressure jump up to 8 MPa. Behind this jump the pressure monotonically increases up to 21 MPa. Since there are many such simultaneous discharges, which have together the same current as the discharge burning from one needle electrode (at the same liquid conductivity), it can be concluded that production of pressure waves by composite electrodes is much more efficient.

The same similarity with needle electrode holds also in the case of *composite cathode*: the pressure profile of wave generated by a discharge from single pore monotonically increases from its outer radius to the pore (without any jump) reaching 20 MPa near the composite cathode surface.

The semi-spherical pressure waves generated by discharges on electrodes of both polarities (on composite anode and cathode) do not often have in one moment (moment of laser-shot generating interferogram) the same radii, probably because each discharge is initiated in slightly different time (due to various filling of pores).

Experiments with focused shockwaves generated by multichannel corona-like discharges on the cylindrical composite anode showed that expanding cylindrical pressure wave, which is formed by many elementary semi-spherical waves produced by surface corona-like discharges, creates after reflection from a parabolic reflector a conical shock wave travelling along the axis of symmetry of the reflector. In the plane of real focus (7.5 mm further than the geometric focus of the reflector) the pressure amplitude of the shock wave rapidly decreases with radial distance from the generator axis; it falls to half of its maximum at 0.25 mm. The pressure waveform also significantly changes with the radial distance. The measured peak pressure of the focused shock wave reaches 372 MPa. The propagation velocity of the conical shock front in its normal direction is $1.51 \pm 0.1\ km \cdot s^{-1}$. The propagation velocity of the vertex of the conical shockwave on the axis of symmetry is at the given geometry $2.17 \pm 0.1\ km \cdot s^{-1}$.

References

[1] T. J. Lewis, "Breakdown Initiating Mechanisms at Electrode Interfaces in Liquids," *IEEE Transactions on Dielectrics and Electrical Insulation,* vol. 10, pp. 948-955, 2003.

[2] A. Starikovskiy, Y. Yang, Y. I. Cho and A. Fridman, "Non-equilibrium plasma in liquid water: dynamics of generation and quenching," *Plasma Sources Sci. Technol.,* vol. 20, p. 7pp, 2011.

[3] V. Y. Ushakov, Impulse Breakdown of Liquids, Heidelberg: Springer-Verlag, 2007.

[4] A. Denat, "High Field Conduction and Prebreakdown Phenomena in Dielectric Liquids," *IEEE Transactions on Dielectrics and Electrical Insulation,* vol. 13, pp. 518-525, 2006.

[5] M. Pekker, Y. Seepersad, M. N. Shneider, A. Fridman and D. Dobrynin, "Initiation stage of nanosecond breakdown in liquid," *J. Phys. D: Appl. Phys.,* vol. 47, p. 025502, 2014.

[6] M. N. Shneider and M. Pekker, "Dielectric fluid in inhomogeneous pulsed electric field," *Phys. Rev.,* vol. 87, p. 043004(7), 2013.

[7] Y. Seepersad, M. Pekker, M. N. Shneider, D. Dobrynin and A. Fridman, "On the electrostrictive mechanism of nanosecond-pulsed breakdown in liquid phase," *J. Phys. D: Appl. Phys.,* vol. 46, p. 162001(6), 2013.

[8] Y. Seepersad, M. Pekker, M. N. Shneider, A. Fridman and D. Dobrynin, "Investigation of positive and negative modes of nanosecond pulsed discharge in water and electrostriction model of initiation," *J. Phys. D,* vol. 46, p. 355201, 2013.

[9] P. Bruggeman, J. Degroote, C. Leys and J. Vierendeels, "Plasma Characteristics in Air and Vapor Bubbles in Water," in *proceedings of the 28th International Conference on Phenomena in Ionized Gases,* Prague, 2007.

[10] K. Tachibana, Y. Takekata, Y. Mizumoto, H. Motomura and M. Jinno, "Analysis of a pulsed discharge within single bubbles in water under synchronized conditions," *Plasma Sources Sci. Technol.,* vol. 20, p. 034005 (12), 2011.

[11] P. Bruggeman, D. Degroote, J. Vierendeels and C. Leys, "DC-excited Discharges in Vapour Bubbles in Capillaries," *Plasma Sources Sci. Technol.,* vol. 17, p. 025008 (7), 2008.

[12] W. An, K. Baumung and H. Bluhm, "Underwater Streamer Propagation Analyzed from Detailed Measurements of Pressure Release," *J. Appl. Phys.,* vol. 101, p. 053302(10), 2007.

[13] J. F. Kolb, R. P. Joshi, S. Xiao and K. H. Schoenbach, "Streamers in Water and Other Dielectric Liquids," *J. Phys. D: Appl. Phys.,* vol. 41, p. 234007 (22), 2008.

[14] P. Bruggeman and C. Leys, "Non-thermal Plasmas in And in Contact with Liquids," *J. Phys. D: Appl. Phys.,* vol. 42, p. 053001(28), 2009.

[15] L. Bok-Hee, K. Dong-Seong and C. Jong-Hyuk, "Underwater Discharge Phenomena in Inhomogeneous Electric Fields Caused by Impulse Voltages," *Journal of Electrical Engineering & Technology,* vol. 5, pp. 329-336, 2010.

[16] P. Ceccato, "Filamentary Plasma Rischarge Inside Water : Initiation and Propagation of a Plasma in a Dense Medium," Phd Report, 2009.

[17] I. M. Gavrilov, V. R. Kukhta, V. V. Lopatin and P. G. Petrov, "Dynamics of Prebreakdown Phenomena in a Uniform Field in Water," *IEEE Transactions on Dielectrics and Electrical Insulation,* vol. 1, pp. 496-502, 1994.

[18] P. Sunka, V. Babicky, M. Clupek, M. Fuciman, P. Lukes, M. Simek, J. Benes, B. R. Locke and Z. Majcherova, "Potential Applications of Pulse Electrical Discharges in

Water," *Acta Phys. Slovaca,* vol. 54, no. 2, pp. 135-145, 2004.

[19] P. Sunka, V. Babicky, M. Clupek, J. Benes and P. Pouckova, "Localized damage of tissues induced by focused shock waves," *IEEE Trans. Plasma Sci.,* vol. 32, no. 4, pp. 1609 - 1613, 2004.

[20] P. Lukes, M. Clupek, V. Babicky and P. Sunka, "Pulsed Electrical Discharge in Water Generated Using Porous-Ceramic-Coated Electrodes," *IEEE Transactions on Plasma Science,* vol. 36, pp. 1146-1147, 2008.

[21] V. Stelmashuk and P. Hoffer, "Shock Waves Generated by an Electrical Discharge on Composite Electrode Immersed in Water With Different Conductivities," *IEEE Transactions on Plasma Science,* vol. 40, no. 7, pp. 1907-1912, 2012.

List of publications

Publications in refereed journals with impact factor (excerpted from WOS):

P. Lukes, P. Sunka, P. Hoffer, V. Stelmashuk, P. Pouckova, M. Zadinova, J. Zeman, L. Dibdiak, H. Kolarova, K. Tomankova, S. Binder, J. Benes, "Focused tandem shock waves in water and their potential application in cancer treatment," *Shock Waves*, vol. 24, no. 1, pp. 51-57, 2014.
Number of citation: 0

V. Stelmashuk and P. Hoffer, "Shock Waves Generated by an Electrical Discharge on Composite Electrode Immersed in Water With Different Conductivities," *IEEE Transactions on Plasma Science*, vol. 40, no. 7, pp. 1907-1912, 2012.
Number of citation: 2

Chapter in book (excerpted from Scopus):

P. Lukeš, P. Šunka., P, Hoffer, V. Stelmashuk, J. Beneš, P. Poučková, M. Zadinová, J. Zeman, "Generation of Focused Shock Waves in Water for Biomedical Applications.", *Plasma for Bio-Decontamination, Medicine and Food Security*. Netherlands: Springer, 2012. 403-416. ISBN 978-94-007-2851-6
Number of citation: 1

Other:

J. Zeman, J. Hach, L. Dibdiak, P. Šunka, P. Lukeš, P. Hoffer, R. Sedláček, K. Kociová, J. Beneš, "Účinek rázové vlny na kostní cement a její potenciální využití v ortopedii," *Ortopedie*, vol. 6, no. 3, pp. 100-102, 2012.

V. Stelmashuk, P. Lukeš, P. Hoffer 2012, "Effect of solution conductivity on shock wave pressure generated by multichannel electrical discharge in water" In Special Session Medical and Biological Applications: *proceedings of the 28th International Symposium on Shock Waves*, ed. K. Kontis, Berlin Heidelberg: Springer Verlag GmbH, pp. 599-604, ISBN 978-3-642-25684-4

P. Lukeš, P. Šunka, P. Hoffer, V. Stelmashuk, J.Beneš, P. Poučková, M. Zadinová, J. Zeman, L. Dibdiak, H. Kolářová, K. Tománková, S. Binder 2012, "Focused tandem shock waves in water and their potential application in cancer treatment" In Special Session Medical and Biological Applications: *proceedings of the 28th International Symposium on Shock Waves*, ed. K. Kontis, Berlin Heidelberg: Springer Verlag GmbH, pp. 839-845, ISBN 978-3-642-25684-4

P. Hoffer, P. Šunka, P. Lukeš 2011, "Dynamics of cavitation induced by focused tandem shock waves in water" In Physics of Plasmas and Ionized Media: *proceedings of the 20th Annual Conference of Doctoral Students*, eds. J. Šafránková, J. Pavlů, Praha : Matfyzpress, pp. 267-272, ISBN 978-80-7378-185-9

P. Hoffer, P. Sunka, P. Lukes, V. Stelamshuk 2011, "Cavitation induced by tandem shock waves" In oral presentation at *2011 International Bioelectrics Symposium*, Toulouse.

P. Hoffer 2010, "Interaction of cavitations with tandem shockwaves in water" In *proceedings of the 14th International Student Conference on Electrical Engineering*, POSTER 2010, Praha.

P. Hoffer, P. Šunka, V. Stelmashuk 2009, "Dynamics of cavitations induced by tandem shock waves in water" In *proceedings of the 29th International Conference on Phenomena in Ionized Gases*, eds. J. de Urquijo, A. Juarez, Cancun, Mexico : Institute of Physics, PA4-5-8. ISBN: 978-1-61567-694-1

P. Lukeš, P. Šunka, M. Člupek, V. Babický, P. Hoffer, M. Šimek, V. Stelmashuk, "Elektrické výboje ve vodě a jejich využití k čištění vody a v medicíně," *Československý časopis pro fyziku*. Roč. 59, č. 4, s. 202-206, 2009.

The contributions of co-authors were equal in all cases

List of projects

2013-2016 Optimalizace účinnosti generace a transportu ozonu. Poskytovatel: Technologická agentura České republiky; ID projektu: TA03010098.
Spoluřešitel

2014-2016 Chemické procesy vyvolané výbojovým plazmatem ve vodných roztocích a jejich využití pro nové aplikace. Poskytovatel: Ministerstvo školství, mládeže a tělovýchovy; ID projektu: *LD14080.
Spoluřešitel

2013-2015 Nové zdroje atmosférického plazmatu na bázi povrchových bariérových výbojů pro biomedicínské aplikace. Poskytovatel: Ministerstvo školství, mládeže a tělovýchovy; ID projektu: LD13010.
Spoluřešitel

2012-2015 Charakterizace fyzikálních a chemických procesů ve výbojovém plazmatu ve vodě pro biologické a biomedicínské aplikace. Poskytovatel: Akademie věd České republiky; ID projektu: *M100431203.
Spoluřešitel

2012-2015 Laboratorní výboje pro simulace a výzkum atmosférických TLE jevů. Poskytovatel: Akademie věd České republiky; ID projektu: M100431201.
Spoluřešitel

2009-2011 Dvě po sobě následující fokusované rázové vlny a jejich potenciální využití v terapii nádorů a řízeném uvolňování léčiv. Poskytovatel: Grantová agentura České republiky; ID projektu: GA202/09/1151.
Spoluřešitel

2006-2008 Záření impulsních silnoproudých výbojů stabilizovaných blízkou stěnou. Poskytovatel: Grantová agentura České republiky; ID projektu: GA202/06/1324.
Spoluřešitel

Résumé

Dizertační práce se zabývá koroně podobnými výboji ve vodě a v solných roztocích, a produkcí rázových vln těmito výboji. Práce obsahuje tři experimentální části.
První experimentální část se zabývá analýzou procesu vzniku míst se silným elektrickým polem na rozhraní elektrického výboje a kapalné elektrody (na hladině). Z těchto míst se následně šíří do objemu kapaliny výbojové strimery. Tento proces je studován na hladině kapalných elektrod (obou polarit), kde dochází k pronikání elektrického výboje z prostoru plynného skupenství skrz rozhraní (hladinu) do objemu kapalné elektrody. Analýza ukázala, že vznik strimeru z vodní hladiny je limitován vodivostí kapaliny. Byl navržen mechanizmus, který dává vznik strimeru do souvislosti s poměrem vodivosti plazmatu u vodní hladiny a vodivosti kapaliny. Dále bylo zjištěno, že pravděpodobnost vzniku strimeru je značně závislá na použité polaritě; vznik sekundárního (kladného) strimeru vyžaduje o řád vyšší intenzitu elektrického pole u hladiny kapalné katody (~10 $MV \cdot m^{-1}$) než vznik záporného strimeru u hladiny kapalné anody (~1 $MV \cdot m^{-1}$).
Druhá experimentální část je věnována analýze tlakového pole okolo koroně podobných výbojů na vodivých hrotech, a okolo výbojů na povrchu kompozitních elektrod. Hlavním diagnostickým nástrojem byl Mach-Zehnderův interferometr pracující ve viditelné oblasti. Podobná analýza byla dříve provedena jen v okolí sekundárních strimerů. Analýza tlakového pole okolo výbojů na kompositních elektrodách nebyla dosud provedena vůbec. Podařilo se analyzovat tlakové pole okolo primárních strimerů na hrotové anodě, a okolo záporných strimerů na hrotové katodě. V okolí primárních strimerů byla zachycena kulová rázová vlna s tlakem 33 MPa při poloměru 0.1 mm. V okolí záporných strimerů je tlakové pole prostorově spojité s maximem 20 MPa na konci strimeru. V případě výbojů ve vodních roztocích NaCl (0.4 $S \cdot m^{-1}$, 0.8 $S \cdot m^{-1}$, 1.8 $S \cdot m^{-1}$, a 3.8 $S \cdot m^{-1}$) se projevuje značný vliv polarity na vývoj výbojového kanálu; zatímco výboje na záporných hrotech produkují při všech zvolených vodivostech expandující dutinu zhruba kulového tvaru, výboje na kladných hrotech vytvářejí množství dlouhých výbojových kanálů produkujících složité tlakové pole. Tlakové pole okolo záporných výbojů tak bylo analyzováno při všech vodivostech, u výbojů na kladných hrotech to bylo možné pouze při vodivostech 1.8 $S \cdot m^{-1}$ a 3.8 $S \cdot m^{-1}$. V případě kladných výbojů byly zachyceny kulové tlakové vlny s poloměrem okolo 1 mm a tlakem menším než 25 MPa. Kulové tlakové vlny produkované zápornými výboji dosahují při srovnatelných poloměrech méně než polovičního maximálního tlaku. Tlakové pole okolo výbojů na povrchu kompositních elektrod bylo provedeno při vodivosti solného roztoku 1.8 $S \cdot m^{-1}$. Výboje produkují kulové tlakové vlny (do poloprostoru) s amplitudou srovnatelnou s vlnami na hrotech. Při stejném proudu odebíraném ze zdroje však produkují desítky takových vln – produkce tlakových vln kompozitními elektrodami je proto účinnější.
Třetí experimentální část se zabývá analýzou tlakového pole v ohnisku generátoru rázových vln, využívajícího kompositní anodu jako zdroje válcové tlakové vlny, která je po odrazu od parabolického reflektoru (katoda) transformována na rázovou vlnu. Mapování tlakového pole již bylo v minulosti provedeno pomocí zastaralých metod (použitím PVDF tlakových senzorů a šlírové metody). Nyní byl k měření tlaku použit optický hydrofon (fiber optic probe hydrophone) a rázová vlna byla pozorována metodou stínografie za pomoci rychlé kamery. Ukázalo se, že v ohnisku reflektoru vzniká kuželová rázová vlna s vrcholem na ose reflektoru. Vrchol kuželové vlny se šíří podél osy reflektoru rychlostí 2.17 $km \cdot s^{-1}$, a tlak rázové vlny na ose v okolí ohniska reflektoru dosahuje hodnoty 372 MPa.